

A Switching Controller for Piezoelectric Microactuators in Dual-Stage Actuator Hard Disk Drives

Jinchuan Zheng¹ and Minyue Fu²

Abstract—Dual-stage actuators (DSAs) with piezoelectric (PZT) microactuators can provide faster track seeking and more accurate track following in hard disk drives (HDDs) than conventional single-stage actuators. However, one of the control challenges of the DSA systems is the PZT actuator saturation. To avoid saturating the PZT actuator, most of the existing methods either carefully design the PZT controllers with small gains or limit the amplitudes of the reference commands. This typically leads to performance conservation because the fast dynamics of the PZT is not fully utilized. Unlike the existing methods, this paper studies a switching controller that optimizes a quadratic performance cost function involving the PZT saturation model explicitly. The controller can not only guarantee the system stability in the presence of saturation but also improve the tracking speed by efficiently allocating the control efforts. Simulation results show the effectiveness of the switching controller with faster disturbance rejection.

I. INTRODUCTION

In recent years, dual-stage actuators (DSAs) with piezoelectric (PZT) microactuators have been adopted in commercial high-performance hard disk drives (HDDs) to meet the ever increasing demands for high-capacity and fast data rate. The mechanism of the DSA structure [1] is simple and of low cost, which makes it feasible in mass production. However, the control design of the DSA systems imposes more challenges than conventional single-stage voice coil motor (VCM) systems mainly because of the PZT actuation redundancy versus single controlled output [the so-called position error signal (PES)]. In other words, for a given desired trajectory, alternative inputs to the two actuators are not unique. Thus, a proper control strategy is required for control allocation in response to external inputs. Otherwise, the two actuators may fight each other and deteriorate the performance instead. One of the control strategies that are popularly used is the decoupled master-slave control [2], where the PZT actuator is aimed at following the position error of the VCM actuator. The other is the PQ design method [3], where the VCM actuator is allocated to response to low frequency components of the system input while the PZT actuator to high frequency components due to its faster dynamics. Moreover, according to the classification of the control tasks in HDDs, control design for track following and settling can be also found in [3]–[5]. In [6], a decoupled track-seeking controller using a three-step design approach is

developed to enable high-speed one-track seeking and short-span track-seeking for a dual-stage servo system. Further, short and long-span seeking controls are incorporated in a single control scheme with fast settling time [7], [8].

Although the PZT microactuator has a faster dynamics in response to external inputs, its drawback is the very limited stroke relative to the VCM actuator. In the point of view of control system, this can be regarded as an actuator saturation problem. It is shown that if the controller cannot handle the PZT saturation properly, the system output will have significant oscillations or even lead to potential instability [9]. Therefore, to avoid saturating the PZT actuator, most of the existing controllers attempts to limit the PZT controller gain such that the PZT actuator works in its linear region only. In such methods, the PZT saturation model is not taken into account in the control design process and thus leading to performance conservations such as reduced servo bandwidth of the PZT actuator. In [9], the authors developed a modified decoupled master slave dual-stage control scheme by simply using a nonlinear PZT model with saturation nonlinearity in its observer and showed its improvement on the stability against the saturation. In this paper, we will discuss a switching control scheme [10], [11] for the PZT actuator which can not only guarantee the system stability in the presence of saturation but also improve the tracking performance by efficiently allocating the control efforts.

In our design, we explicitly model the PZT actuator as a saturated actuator whose control problem is then casted as a linear quadratic control problem with input saturation. The solution of the problem eventually leads to a switching controller. Unlike the anti-windup compensator [12] that uses ad-hoc methods to detune the controller with little theoretical guarantee on stability, the switching control scheme can not only guarantee the stability in the presence of saturation, but also optimize a quadratic performance function through properly over-saturating the controller that leads to desired fast convergence of the tracking error.

II. SYSTEM MODEL AND CONTROL STRUCTURE

Fig. 1 shows a typical DSA with a push-pull PZT microactuator in hard disk drives. It consists of a VCM actuator as the primary stage and a PZT actuator as the secondary stage. The PZT is located between the suspension and the E-block, which is moved by the VCM. The two actuators are respectively driven through a PZT amplifier and a VCM driver. The VCM driver has a voltage input limit of ± 3.5 V. The PZT actuator has a stroke limit of ± 0.5 μm and the PZT amplifier has a voltage input limit of ± 1.5 V.

¹J. Zheng is with the Faculty of Engineering and Industrial Sciences, Swinburne University of Technology, Hawthorn, VIC 3122, Australia jzheng@swin.edu.au

²M. Fu is with the School of Electrical Engineering and Computer Science, The University of Newcastle, Callaghan, NSW 2308, Australia Minyue.Fu@newcastle.edu.au

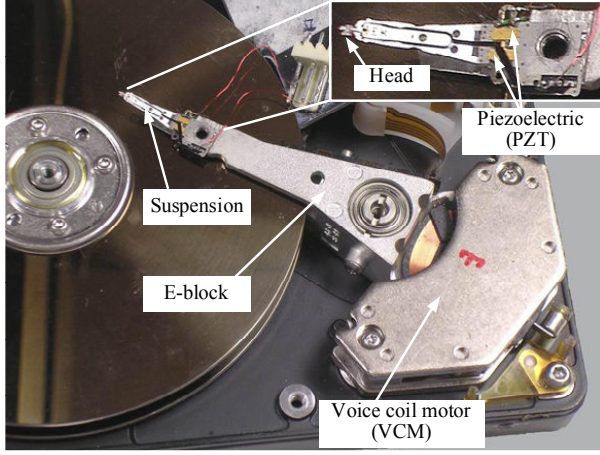


Fig. 1. A hard disk drive using dual-stage actuator with piezoelectric microactuator.

Under the assumption that the coupling effects between the two actuators are negligible, the DSA plant model of the DSA can be regarded as a decoupled dual-input and single-output system. Moreover, we assume notch filters have been cascaded to the VCM and PZT actuators to actively damp their resonances, respectively (see our work in [8] for details). As such, a control-oriented model of the DSA system can be described by Fig. 2, where the state-space equations of VCM and PZT actuator is given by

$$\begin{cases} \Sigma_1 : \dot{x}_1 = A_1 x_1 + B_1 \sigma(u_1), & x_1(0) = 0 \\ \Sigma_2 : \dot{x}_2 = A_2 x_2 + B_2 \sigma(u_2), & x_2(0) = 0 \\ y = y_1 + y_2 = C_1 x_1 + C_2 x_2 \end{cases} \quad (1)$$

where the state $x_1 = [y_1 \ \dot{y}_1]^T$, $x_2 = [y_2 \ \dot{y}_2]^T$,

$$A_1 = \begin{bmatrix} 0 & 1 \\ 0 & 0 \end{bmatrix}, B_1 = \begin{bmatrix} 0 \\ b_1 \end{bmatrix}, C_1 = [1 \ 0],$$

$$A_2 = \begin{bmatrix} 0 & 1 \\ a_1 & a_2 \end{bmatrix}, B_2 = \begin{bmatrix} 0 \\ b_2 \end{bmatrix}, C_2 = [1 \ 0],$$

and the saturation function $\sigma(u_i)$ ($i = 1, 2$) is defined as

$$\sigma(u_i) = \text{sgn}(u_i) \min\{\bar{u}_i, |u_i|\} \quad (2)$$

where \bar{u}_i is the saturation level of the i th control input. The DSA model parameters in (2)-(2) are given by

$$b_1 = 1.7 \times 10^8, \quad a_1 = -10^9, \quad a_2 = -3.1 \times 10^4, \\ b_2 = 4.3 \times 10^8, \quad \bar{u}_1 = 3 \text{ V}, \quad \bar{u}_2 = 1.25 \text{ V}.$$

As mentioned earlier, the control strategies for the coordination of the two actuators are not unique as the DSA system is a dual-input single-output system. Here, we use the decoupled master-slave control structure because it offers the benefit that the overall stability of the DSA loop can be guaranteed by independently stabilized VCM loop and PZT loop. This control structure is shown in Fig. 3, where the system input is the disturbance d . The control objective to

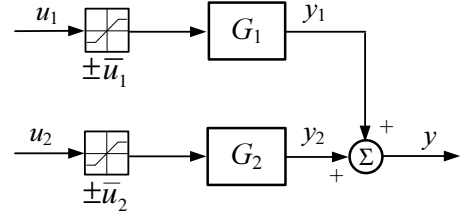


Fig. 2. A control-oriented model of the DSA system. G_1 : VCM model, G_2 : PZT model.

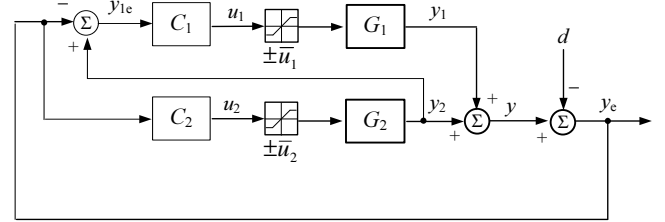


Fig. 3. Block diagram of DSA control system. d : disturbance input; y_e : the overall position error signal; y_{1e} : the VCM position error signal.

regulate the position error signal y_e swiftly and as small as possible.

From Fig. 3, it is easy to find that the VCM position error y_{1e} equals to

$$\begin{aligned} y_{1e} &= y_2 - y_e \\ &= d - y_1 \end{aligned} \quad (3)$$

and when combined with the VCM feedback controller C_1 , we have

$$y_{1e} = \frac{1}{1 + G_1 C_1} d. \quad (4)$$

We can see that the VCM loop is decoupled from the PZT loop and C_1 can be designed using any conventional methods and is thus not detailed here because it is not the primary goal of this paper. Typically, due to the relatively slow dynamic characteristics of the VCM, we can only expect $|y_{1e}| \leq \varepsilon$, ($\varepsilon > 0$) for any persistent bounded disturbance input. It follows that the PZT control effort u_2 should be designed to compensate for the residual VCM position error, i.e., driving $y_2 = y_{1e}$. If this can be achieved, it immediately implies that $y_e = y_2 - y_{1e} = 0$.

To formulate the control problem of the PZT actuator, define $w_1 = y_e$ and $\dot{w}_1 = w_2 = \dot{y}_2 - \dot{y}_{1e}$, then

$$\dot{w}_2 = a_1 w_1 + a_2 w_2 + b_2 (\sigma(u_2) - f), \quad (5)$$

where $f = (\ddot{y}_{1e} - a_2 \dot{y}_{1e} - a_1 y_{1e})/b_2$. We observe that the coupling signal $f(t)$ is dominated by the VCM position error dynamics. Intuitively, it is only when the VCM drives $f(t)$ to converge to a small region within the PZT's control limit that the PZT can make some meaningful control effort. In view of this, we assume that the VCM control loop is well designed such that $|f(t)| \leq f_0, \forall t \geq 0$ and $f_0 < \bar{u}_2$. Under this circumstance, we can introduce a feedforward input in u_2 as follows:

$$u_2 = u + f \quad (6)$$

such that $f(t)$ is compensated. Then, we can formulate the PZT control design as a regulation control problem with input saturation and the system model (5) can be rewritten as follows:

$$\dot{x} = Ax + B\sigma(u), \quad x(0) = x_0 \quad (7)$$

where $x = [w_1 \ w_2]'$, $A = A_2$, $B = B_2$, and $\sigma(\cdot)$ with saturation level equal to 1. In the next section, we will discuss a switching control design for the PZT control input u .

III. SWITCHING CONTROL DESIGN

In this section, we first introduce the fundamental theory of a linear quadratic saturation control design. Next, a switching controller is developed based on the saturation control design method, which offers performance improvement. Finally, we present the design result of the switching controller with application to the PZT actuator.

A. Saturation Control Design

Consider the system in (7), we first introduce the following quadratic cost function

$$J(x_0, u) = \int_0^\infty (x^T Q x + r\sigma(u)^2) dt \quad (8)$$

for some $Q = Q^T > 0$ and $r > 0$ with (A, B) being controllable. Ideally, we aim to seek an optimal linear state feedback

$$u = Kx \quad (9)$$

for each given initial state x_0 such that $J(x_0, u)$ is minimized. It is well-known that if the control is not saturated, the optimal solution to K is given by

$$K = -r^{-1}B^T P_0 \quad (10)$$

where $P_0 = P_0^T > 0$ is the solution to the following Riccati equation

$$A^T P_0 + P_0 A + Q - r^{-1}P_0 B B^T P_0 = 0 \quad (11)$$

Moreover, the minimal cost is given by $x_0^T P_0 x_0$.

However, in the presence of saturation, the optimal K is difficult to give. To overcome this difficulty, we parameterize the controller by using an optimal sector bound [10]. More specifically, define the level of over-saturation $\rho \geq 0$ such that the control input u is restricted to be

$$|u| \leq 1 + \rho \quad (12)$$

It is easy to verify that for any u constrained by (12), $\sigma(u)$ lies in the following sector bound

$$\sigma(u) = \rho_1 u + \delta(u) \quad (13)$$

$$|\delta(u)| \leq \rho_2 u, \quad \forall |u| \leq 1 + \rho \quad (14)$$

where

$$\rho_1 = \frac{2 + \rho}{2(1 + \rho)}, \quad \rho_2 = \frac{\rho}{2(1 + \rho)} \quad (15)$$

Here, ρ_1 is the optimal value so that $\delta(u)$ has the smallest sector to bound the nonlinearity cause by the saturation.

Now, we give some analysis on the design of a control gain K to minimize the worst-case cost for all $\delta(\cdot)$ satisfying the sector bound (14). For a given $\rho > 0$, consider the Lyapunov function candidate

$$V(x) = x^T P_\rho x, \quad P_\rho = P_\rho^T > 0 \quad (16)$$

and define

$$\Omega_\rho = A^T P_\rho + P_\rho A + Q - r^{-1}P_\rho B B^T P_\rho, \quad (17)$$

$$u^* = -r^{-1}B^T P_\rho x \quad (18)$$

Given any initial state x_0 and any $\delta(\cdot)$ satisfying (14), it is easy to verify that

$$\begin{aligned} J(x_0, u, T) &= \int_0^T (x^T Q x + r\sigma(u)^2) dt \\ &= V(x_0) - V(x(T)) \\ &\quad + \int_0^T \left(\frac{d}{dt} V(x) + x^T Q x + r\sigma(u)^2 \right) dt \\ &\leq V(x_0) + \int_0^T g(x, u, \delta(u)) dt \end{aligned}$$

where

$$g(x, u, \delta(u)) = x^T \Omega_\rho x + r(\rho_1 u + \delta(u) - u^*)^2 \quad (19)$$

This implies that if $g(x, u, \delta(u)) \leq 0$ for all $x \in \mathbb{R}^n$ and $\delta(\cdot)$ satisfying (14), then

$$J(x_0, u) \leq V(x_0) \quad (20)$$

From the analysis above, we formulate the following relaxed optimal control problem:

PI: For a given $\rho \geq 0$, design P_ρ and u to minimize $V(x_0)$ subject to $g(x, u, \delta(u)) \leq 0$ for all $x \in \mathbb{R}^n$ and $\delta(\cdot)$ satisfying (14). Moreover, determine the largest invariant set X_ρ characterized by an ellipsoid of the form

$$X_\rho = \{x : x^T P_\rho x \leq \mu_\rho^2\}, \quad \mu_\rho > 0 \quad (21)$$

such that if $x_0 \in X_\rho$, $x(t) \in X_\rho$ and $|u(t)| \leq 1 + \rho$ for all $t \geq 0$, we have $J(x_0, u) \leq V(x_0)$.

The solution to the above problem is given by the following Theorem:

Theorem 1 [10]: Consider the system in (7) and the cost function in (8). For a given level of over-saturation $\rho \geq 0$, suppose the equation

$$A^T P_\rho + P_\rho A + Q - r^{-1}(1 - \rho_0^2)P_\rho B B^T P_\rho = 0 \quad (22)$$

where

$$\rho_0 = \frac{\rho_2}{\rho_1} = \frac{\rho}{2 + \rho} \quad (23)$$

has a solution $P_\rho = P_\rho^T > 0$. Then the optimal feedback control law K_ρ for the relaxed optimal control problem *PI* is given by

$$K_\rho = -\rho_1^{-1}r^{-1}B^T P_\rho \quad (24)$$

and the associated invariant set X_ρ is bounded by

$$\mu_\rho = \frac{r}{(1 - \rho_0)\sqrt{B^T P_\rho B}} \quad (25)$$

Remark 1: If $\rho = 0$, the Riccati equation (22) and the control law (24) recover the results in (11) and (10) for optimal control without saturation. The associated invariant set is given by

$$X_0 = \{x : x^T P_0 x \leq \mu_0^2\}, \quad \mu_0 = \frac{r}{\sqrt{B^T P_0 B}} \quad (26)$$

Remark 2: Taking $\rho \rightarrow \infty$ (or equivalently, $\rho_0 \rightarrow 1$) and solving for P_ρ in (22) gives the largest invariant set as

$$X_\infty = \{x : x^T P_\rho x < \mu_\infty^2\} \\ \mu_\infty = \frac{r}{(1 - \rho_0)\sqrt{B^T P_\rho B}}, \quad \rho_0 \rightarrow 1 \quad (27)$$

Note that the solvability of P_ρ for any $\rho > 0$ is guaranteed by the controllability of (A, B) and positive definiteness of Q .

Remark 3: Despite that the invariant set enlarges when ρ increases, it can be seen that the upper bound of the performance cost in (20) is as well larger. This implies that the saturated controller can bring a good benefit when ρ is not close to 0 and not too large. Generally, ρ can be selected as the minimal one satisfying $x_0 \in X_\rho$.

1) *Property of the control law:* The proposed controller in Theorem 1 has two nice properties, i.e., the nesting property of X_ρ and monotonicity of P_ρ . More specifically, define

$$S_\rho = (1 - \rho_0)P_\rho \quad (28)$$

We can rewrite the Riccati equation in (22) as

$$A^T S_\rho + S_\rho A + (1 - \rho_0)Q - r^{-1}(1 + \rho_0)S_\rho B B^T S_\rho = 0 \quad (29)$$

and the invariant set can be expressed as

$$X_\rho = \{x : x^T S_\rho x \leq \frac{r^2}{B^T S_\rho B}\} \quad (30)$$

Lemma 1 [10]: The solution S_ρ to (29) is monotonically decreasing in $\rho > 0$, i.e., for a sufficiently small $\epsilon > 0$, $S_\rho > S_{\rho+\epsilon}$, if $0 \leq \rho < \rho + \epsilon$. Consequently, X_ρ are nested in the following sense:

$$X_\rho \subset X_{\rho+\epsilon}, \quad \forall 0 \leq \rho < \rho + \epsilon \quad (31)$$

Moreover, the solution P_ρ to the Riccati equation in (22) is monotonically increasing in $\rho > 0$. That is,

$$P_\rho < P_{\rho+\epsilon}, \quad \forall 0 \leq \rho < \rho + \epsilon. \quad (32)$$

B. Switching Control

Thanks to the nesting property of X_ρ and monotonicity of P_ρ , we can apply Theorem 1 to design a sequence of control gains K_i , based on which a nested switching control can be developed to improve the performance. More specifically, choose a sequence of over-saturation bounds $0 = \rho_0 < \rho_1 < \dots < \rho_N$ and solve the corresponding Lyapunov matrices P_i , invariant sets X_i and controller gains K_i , $i = 0, 1, \dots, N$. We then construct the nested switching control law by selecting the control gain K_i when $x \in X_i$ and $x \notin X_{i-1}$ (unless $i = 0$). The following result shows the advantage of the nested switching control in the performance improvement.

Lemma 2: Suppose the switching controller above is applied to the system in (7) with $x_0 \in X_N$. Let t_i be the time instance K_i is switched on, $i = 0, 1, \dots, N$, particularly, $t_N = 0$. Then the cost of the switching control is bounded by

$$J(x_0, u) \leq x_0^T P_N x_0 - \sum_{i=0}^{N-1} x^T(t_i)(P_{i+1} - P_i)x(t_i) \\ < x_0^T P_N x_0. \quad (33)$$

Proof: According to the proof of Theorem 1 [10], we have

$$x^T Q x + r\sigma(K_i x)^2 \leq -\frac{d}{dt}V_i(x) = -\frac{d}{dt}(x^T P_i x) \quad (34)$$

along the trajectory of $x(t)$, where $t \in [t_{i+1}, t_i]$. Following the monotonicity of P_i and integrating the inequality above yields (33).

From the theorem above, we can clearly see the advantage of the switching control by means of the negative term in (33) that decreases the cost gradually. In what follows, we will discuss the application of this switching control scheme to the design of the PZT controller for improved tracking performance.

C. Controller Design for PZT Actuator

Our main purpose here is to use the switching controller for the PZT to expedite the convergence of the position error (y_e) at the presence of the output disturbance d . Particularly, we suppose that the disturbance is a shock wave with an amplitude larger than the PZT's stroke. This scenario generally occurs when the HDDs are used in mobile environment. If the servo controller cannot compensate for the shock disturbance quickly within a small time frame, the read/write head has to wait for a few more revolutions until the head is regulated to the desired sector. This obviously decreases the data throughput. To improve this situation, it is intuitive to inject the maximum control input to the PZT actuator (by applying a large control gain K_i , $i > 0$) to achieve the fastest acceleration at the initial stage. Then the control input should be gradually decreased (by applying a relatively small control gain K_0) to achieve appropriate robustness when the position error approaches zero. Such a control strategy would impose some conditions on Q , r and ρ_i . The switching controller design results for the PZT are given as follows.

First, we design the control gain K_0 (i.e., $\rho_0 = 0$). Under this circumstance, the position error y_e is close to zero and the control input u is not saturated. It is straightforward to verify that the closed-loop system is a linear system and can be expressed as

$$\dot{x} = (A - B B^T P_0)x \quad (35)$$

Clearly, we can select Q and r (hence corresponding to a unique solution of P_0) such that the dominated poles of $A - B B^T P_0$ leads to desired characteristics. More specifically, we first set $r = 1$ without loss of generality since the performance cost can be normalized as J/r . Then, let the

desired poles for the closed-loop system matrix $A - BB^T \bar{P}_0$ be $(-\zeta \pm j\sqrt{1 - \zeta^2})\omega$, where ζ represents the damping ratio and ω the natural frequency. We then parameterize Q as

$$Q = \begin{bmatrix} q_1 & 0 \\ 0 & q_2 \end{bmatrix} \quad (36)$$

with

$$q_1 = \frac{1}{b_2^2}(\omega^4 - a_1^2) \quad (37)$$

$$q_2 = \frac{1}{b_2^2}(4\zeta^2\omega^2 - 2\omega^2 - 2a_1 - a_2^2). \quad (38)$$

Clearly, to guarantee $Q > 0$ requires ω and ζ satisfying the conditions

$$\omega > \sqrt{|a_1|} \quad (39)$$

$$1 \geq \zeta^2 > \frac{(2a_1 + a_2^2)}{4\omega^2} + 0.5. \quad (40)$$

Substituting Q and $r = 1$ into (22) solves P_ρ as

$$P_\rho = \begin{bmatrix} p_1 & p_2 \\ p_2 & p_3 \end{bmatrix} \quad (41)$$

with

$$p_1 = b^2(1 - \rho_0^2)p_2p_3 - a_2p_2 - a_1p_3 \quad (42)$$

$$p_2 = \frac{a_1 + \sqrt{(1 - \rho_0^2)\omega^4 - \rho_0^2a_1^2}}{b_2^2(1 - \rho_0^2)} \quad (43)$$

$$p_3 = \frac{a_2 + \sqrt{a_2^2 + b_2^2(1 - \rho_0^2)(2p_2 + q_2)}}{b_2^2(1 - \rho_0^2)} \quad (44)$$

Accordingly, the resulting control gain with respect to a given ρ is obtained by

$$K_\rho = -\frac{b_2}{\rho_1}[p_2 \ p_3] \quad (45)$$

To this end, it is easy to verify that the closed-loop system characteristic polynomial for $\rho = 0$ is given by

$$\begin{aligned} \Delta_0(s) &= |sI - A - BK_0| \\ &= s^2 + (b_2^2p_3 - a_2)s + (b_2^2p_2 - a_1) \\ &= s^2 + 2\zeta\omega s + \omega^2 \end{aligned} \quad (46)$$

which yields the poles as specified initially.

Based on the above analytic results, we choose $\omega = 2\pi 6000$, $\zeta = 0.8$, which leads to the following controller:

$$\begin{aligned} K_0 &= -[0.9796 \quad 0.0001], \\ P_0 &= \begin{bmatrix} 2.9262 \times 10^{-4} & 2.2781 \times 10^{-9} \\ 2.2781 \times 10^{-9} & 1.5521 \times 10^{-13} \end{bmatrix}, \\ \mu_0 &= 3.4845 \times 10^{-5}. \end{aligned}$$

Second, we design the saturated controllers K_1 by choosing $\rho = 5$. It follows that

$$\begin{aligned} K_1 &= -[1.8278 \quad 0.0001], \\ P_1 &= \begin{bmatrix} 3.0335 \times 10^{-4} & 2.4795 \times 10^{-9} \\ 2.4795 \times 10^{-9} & 1.8370 \times 10^{-13} \end{bmatrix}, \\ \mu_1 &= 3.6066 \times 10^{-4}. \end{aligned}$$

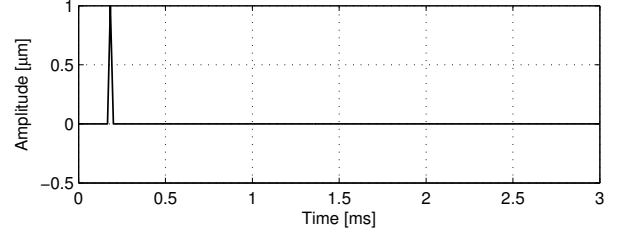


Fig. 4. Shock disturbance signal.

Finally, combining the above two controllers leads to the switching controller as follows:

- $u = 0$ when $[y_e \ \dot{y}_e]P_1[y_e \ \dot{y}_e]^T > \mu_1^2$;
- Controller gain K_1 is switched on when $[y_e \ \dot{y}_e]P_1[y_e \ \dot{y}_e]^T \leq \mu_1^2$ and $[y_e \ \dot{y}_e]P_0[y_e \ \dot{y}_e]^T > \mu_0^2$;
- Controller gain K_0 is switched on when $[y_e \ \dot{y}_e]P_0[y_e \ \dot{y}_e]^T \leq \mu_0^2$.

Note that the control algorithm ensures that there is only one controller active at any time instance.

IV. SIMULATION RESULTS

Simulation is carried out to verify the switching controller. The VCM actuator is simply controlled using a lead-lag controller as follows:

$$C_1(s) = \frac{0.2s^2 + 5236s + 3.298 \times 10^6}{s^2 + 24551s + 1.223 \times 10^8}. \quad (47)$$

We assume that the disturbance signal is with Fig. 4 and the displacement of y_2 can be observed. Then, the simulation results for the designed switching controller are shown in Figs. 5 and 6. We can see that position error of the DSA converges to zero much faster than that of the VCM (see Fig. 6). To clearly see the benefit of the switching scheme, we compare the performance with the non-switching case (i.e., with only the controller K_1). The result is shown in Fig. 7, which indicates a relatively slow settling time instance at 0.5 ms achieved by the non-switching controller as compared to the switching case at 0.35 ms shown in Fig. 6. Thus, we can see that although the controller K_1 guarantees the stability of the system in the presence of saturation, it cannot improve the performance without switching to K_0 that is specifically designed to work around the origin. On the other side, we simulate the result using a proportional controller for the PZT actuator. This is a conventional method [9] by simply ignoring the saturation in the design. Fig. 8 shows that in our specific case when the PZT is saturated, the position error of the DSA achieved by the conventional controller contains significant oscillations and thus results in tedious settling time. Therefore, we conclude that the switching controller can offer the benefit of guaranteed stability through K_1 and fast convergence through K_0 .

V. CONCLUSIONS

This paper developed a switching controller for the PZT actuator in DSA systems for HDDs. The advantage of the

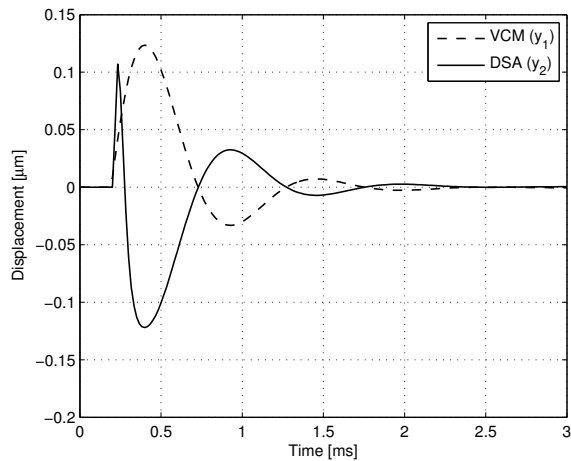


Fig. 5. Displacement signals with switching controller.

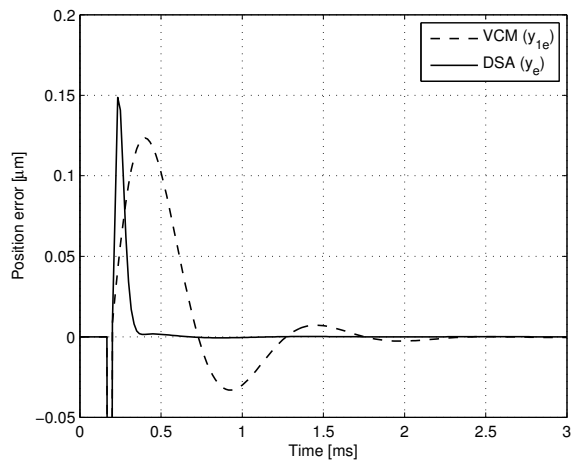


Fig. 6. Position error signals with switching controller.

switching control scheme lies in that the actuator saturation nonlinearity is explicitly considered in the design process such that the closed-loop system stability can be guaranteed in the presence of saturation, meanwhile faster convergence is offered through switching the controllers that optimize a quadratic cost function. The simulation results have shown that the new control scheme can provide faster and more accurate disturbance rejection capability. In future work, we will implement this promising controller on a real experimental platform to evaluate its practical performance.

REFERENCES

- [1] K. Mori, T. Munemoto, H. Otsuki, Y. Yamaguchi, and K. Akagi, "A dual-stage magnetic disk drive actuator using a piezoelectric device for a high track density," *IEEE Trans. Magn.*, vol. 27, no. 6, pp. 5298-5300, Nov. 1991.
- [2] W. Guo, S. Weerasooriya, T. Goh, Q. Li, C. Bi, K. Chang, and T. Low, "Dual-stage actuators for high density rotating memory devices," *IEEE Trans. Magn.*, vol. 34, no. 3, pp. 450-455, Mar. 1998.
- [3] S. Schroeck, W. Messner, and R. McNab, "On compensator design for linear time-invariant dual-input single-output systems," *IEEE/ASME Trans. Mechatron.*, vol. 6, no. 1, pp. 50-57, Mar. 2001.
- [4] X. Huang, and R. Horowitz, "Robust controller design of a dual-stage disk drive servo system with an instrumented suspension," *IEEE Trans. Magn.*, vol. 41, no. 8, pp. 2406-2413, Aug. 2005.

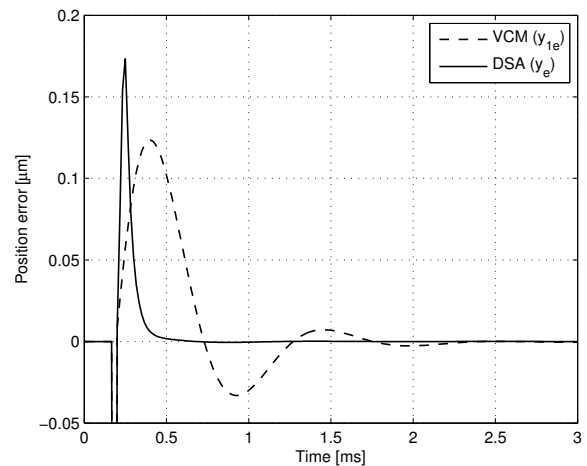


Fig. 7. Position error signals with non-switching controller. The settling time of the DSA position error is much slower than the switching controller as shown in Fig. 6.

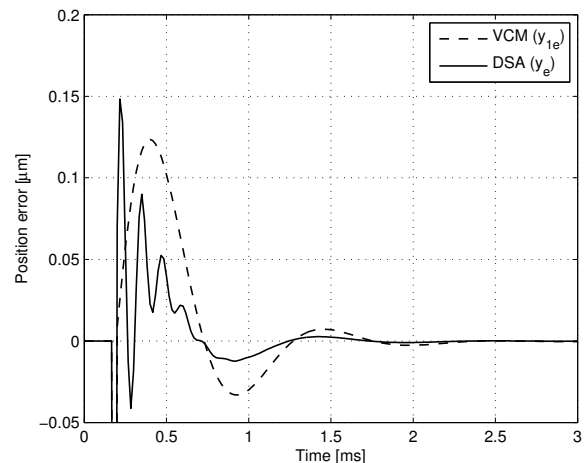


Fig. 8. Position error signals with a conventional PZT controller neglecting the saturation in the design. The DSA position error contains significant oscillations, leading to tedious settling time.

- [5] H. Numasato and M. Tomizuka, "Settling control and performance of a dual-actuator system for hard disk drives," *IEEE/ASME Trans. Mechatron.*, vol. 8, no. 4, pp. 431-438, Dec. 2003.
- [6] M. Kobayashi, and R. Horowitz, "Track seek control for hard disk dual-stage servo systems," *IEEE Trans. Magn.*, vol. 37, no. 2, pp. 949-954, Mar. 2001.
- [7] B. Hredzak, G. Herrmann, and G. Guo, "A proximate-time-optimal control design and its application to a hard disk drive dual-stage actuator system," *IEEE Trans. Magn.*, vol. 42, no. 6, pp. 1708-1715, Jun. 2006.
- [8] J. Zheng, M. Fu, Y. Wang, and C. Du, "Nonlinear tracking control for a hard disk drive dual-stage actuator system," *IEEE/ASME Trans. Mechatron.*, vol. 13, no. 5, pp. 510-518, Oct. 2008.
- [9] G. Guo, D. Wu, and T. Chong, "Modified dual-stage controller for dealing with secondary-stage actuator saturation," *IEEE Trans. Magn.*, vol. 39, no. 6, pp. 3587-3591, Nov. 2003.
- [10] M. Fu, "Linear quadratic control with input saturation," in *Proc. Robust Control Workshop*, Newcastle, Dec. 2000.
- [11] T. Shen, and M. Fu, "High precision and feedback control design for dual-actuator systems," in *Proc. IEEE Conf. Control Applications*, 2005, pp. 956-961.
- [12] N. Kapoor, A. Teel and P. Daoutidis, "An anti-windup design for linear systems with input saturation," *Automatica*, vol.34, pp.559-574, 1998.